J Mater Sci (2007) 42:9343–9354
DOI 10.1007/s10853-007-1878-1

Mechanical testing of disks under gaseous pressure

Calculation of biaxial mechanical properties applications and interests of the testing method

Vladimir Gantchenko · Patrice Jouinot

Received: 4 January 2005 / Accepted: 23 May 2007 / Published online: 28 July 2007

Abstract Numerical calculations are becoming more and more efficient in estimating the lifetime of structures under thermomechanical loading. However, these life estimations cannot be reliable if the necessary parameters have not been correctly identified and measured and if all the causes of damage have not been considered. Disk testing under gas pressure is similar to oil bulging testing. However, disk testing can easily be used for the mechanical characterization of materials subject to more varied solicitations: monotone loading (biaxial rupture tests at strain rates from 10^{-6} to 10^{0} s^{-1}), constant loading under high stresses (sustained load) at elevated temperature (creep tests), cyclic loading (mechanical slow fatigue tests); the temperature may be chosen between 20 and 900 °C and the environment may be studied by comparing the results obtained with either an inert gas or reactive gas. Moreover, disk testing reveals light damage since crossing cracks through the thin membrane create leakages detected by a mass spectrometer. In this paper, we present an original method of calculation developed to determine the true mechanical properties of the pressurized disk; the method of calculation is validated because its numerical results are identical to the measured tensile properties. In addition, the range of uniform deformation is correctly determined; this property is needed to establish sheet formability which is not clearly determined by oil bulging. Of course, the mechanical behaviour can be determined within the whole ranges of temperature and strain rates; such wide ranges cannot be tested by other techniques such as tensile testing or oil bulging. As disk edges are not stressed during testing, the results are very reproducible at any temperature and at any strain rate while the machining or cutting defects initiate very scattered ruptures of tensile specimens tested at high temperature or at high strain rate. The disk and its loading simulate real applications with thin walls embedded by thick parts such as thermal exchangers or spatial engines. The analytical method of calculation may be used for identifying the needed parameters of thermomechanical modelling; it will be optimized by finite elements methods and it would allow a rational quantification of hydrogen embrittlement.

V. Gantchenko · P. Jouinot (✉)
Institut Superieur de Mecanique de Paris (ISMEP),
L.I.S.M.M.A.-Physique des Materiaux, 3 rue Fernand Hainaut,
Saint Ouen 93407, France
e-mail: jouinot@supmeca.fr

Introduction

Finite elements methods (FEM) are increasingly efficient in calculating the elastic and plastic solicitations of mechanical structures and in determining their damage; the calculation methods use mathematical laws for modelling the thermomechanical behaviour of materials.

To obtain correct results by FEM, the thermomechanical laws must be correctly adapted to the structures studied and their solicitations; the associated parameters must be correctly identified and consequently, experimental methods must be chosen to obtain realistic thermomechanical characterizations.

For instance, if thermal exchangers or expansion bellows have to be studied, the damage to their thin walls is more related to the behaviour of thin sheets than to the behaviour of thick specimens; the start-stop cycles of furnaces, thermal engines and turbines create thermal gradients at high rate; the consequent extreme thermomechanical loadings

must be reproduced during the thermomechanical characterization of the materials used.

For about 40 years, disk pressure testing has been used to study hydrogen embrittlement of metals; the results are much more sensitive and reproducible with disk testing than with other embrittlement testing [1–4].

This disk pressure testing has been chosen by the French standard association (AFNOR) in order to qualify the materials of cylinders used as vessels for high-pressure hydrogen [5]; this experimental technique is used in different countries [6–8] and it may become a European standard.

The embrittlement is evaluated by comparing the pressure resistance of disks loaded by either an inert gas or hydrogen; if hydrogen damages the material, it decreases the pressure resistance established with the inert gas.

Disk pressure tests can also be performed in order to determine the mechanical properties of materials subject to biaxial tension such as thin walls of pressure vessels.

This experimental technique is similar to oil bulging [14] but gas loading can be used for characterization at higher temperature or at higher deformation rate than oil loading.

For biaxial testing, the disks are only pressurized under helium and the embrittlement cell has been slightly modified in order to determine easily the intrinsic mechanical properties of the material.

Thus, the actual experimental technique is very sensitive and reproducible to such a degree that the material characterizations are very fine and various; this technique is particularly well adapted for studying the properties of thin walls and several mechanisms or phenomena can be revealed by disk testing while they cannot be revealed by other less sensitive techniques as tensile testing [8–10].

Although the results provided by disk testing are significant and interesting, they are only comparative or qualitative; they cannot be used to calculate the stresses and strains distribution in defined mechanical structures subject to various loadings; of course, the usual tensile testing provides the true mechanical properties needed to calculate such structures but it is not as sensitive as the disk testing in revealing fine phenomena. For that reason, we have developed an analytical method in order to determine the true mechanical properties of the disk material.

Naturally, a new experimental method must be used only if the results have been validated and if they are complementary to established results obtained with other testing methods.

However, the usual mechanical properties of the disk have to be more easily determined with the proposed method than with finite elements methods [11] and the numerous practical and theoretical determinations of strains and stresses in a membrane bulged by a pressurized fluid [12–14] have to be completed and improved.

First, we will describe the experimental technique and the original method developed to determine the mechanical properties of the disk; afterwards, we will present several applications of the disk testing and the associated calculation method in order to show its abilities, interests and advantages.

Experimental technique: biaxial testing of disks

Rupture testing

Before loading, the standard specimen is a flat disk (58 mm in diameter, 0.75 mm in thickness).

The disk is clamped in a cylindrical cell (Fig. 1); embedding begins at 13.25 mm from the disk centre; the disk is loaded by continuously increasing pressure of helium gas until the final rupture or cracking.

NB: Homothetic cells can be used for smaller disks (disk diameter down to 15 mm). The disk thickness may vary between 0.1 and 1 mm.

Moreover, the specimen does not have to be circular; polygons can be cut from material sheets and clamped in the same cylindrical cell.

The embedding radius (r = 4) is great enough to avoid the stress concentration and thus to induce the maximum deformation at the disk pole.

The stresses and the strains are not homogeneous in the disk with the result that the true mechanical properties cannot be easily determined from the experimental results; on the contrary, the disk periphery is not loaded with the

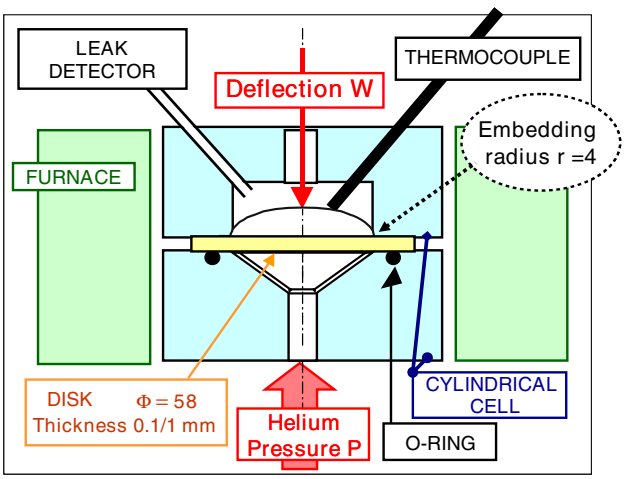

Fig. 1 Cell of biaxial testing. Pressure rate: from 10^{-2} to 2.10^{4} MPa/min, Temperature: from 20 to 900 °C, Smallest leakage: 1 cm^3 Helium/year. The disk is deformed by gaseous helium; the pressure P, the deflection W, the temperature and the flow of helium leakage through the disk are recorded during the disk pressurization

result that local deformations and ruptures are not initiated by edges defects.

The gas is contained in the cell by an elastomer O-ring; for temperatures greater than 150 °C, a metallic O-ring is used.

The loading gas is taken from a high-pressure cylinder (≤150 MPa). The gas flow is regulated by pneumatic valves monitored by a PC-computer [15]; the automated equipment allows tests with loading speeds selected from 10^{-2} to 2.10^4 MPa/min (strain rates from 10^{-6} to 10^0 s^{-1}); such speed ranges are not obtained with only one testing machine.

The mechanical loading is measured using the pressure P and the macroscopic deformation is obtained from the cupola deflection W until the disk ruptures [16].

The disk and the cell can be heated up to 900 °C in an annular furnace; the temperature is measured by a thermocouple on the disk surface.

Very fine helium leakages through the disk can be detected by a mass spectrometer analysing the atmosphere above the disk and measuring the gas flow.

Creep testing

The disk and the cell are heated up to the test temperature; then the cell is rapidly pressurized up to the test pressure; afterwards, the pressure remains constant until the disk ruptures.

During the test, the pressure P and the deflection W are continuously recorded.

Fatigue testing

Identical disks and similar cells are used for fatigue testing: cyclic pressures P_0 and P_1 are applied to the top and bottom faces of the disk; the disk is loaded by the pressure difference $|P_0 - P_1|$, which creates a deflection W alternatively in both directions.

The cycle duration is about 30 s.

Mechanical properties of a pressurized disk

Calculation method

Stresses and strains at the disk pole

The disk becomes a cupola during its deformation; near the cupola pole, the material is subject to the meridian and circumference stresses σ_φ and σ_θ and to the radial stress σ_z in the thickness direction.

At the pole, only the tensile stresses will be calculated because the flexion may be neglected for a thin membrane.

The radial stress σ_z on the inner surface is the gas pressure P; this stress is also neglected because its maximum value is always a small percentage of the other stresses σ_φ and σ_θ.

Thus, the disk pole is subject to plane tensile stresses that reduce its thickness from t_0 to t; the strain ε_z in the thickness direction is calculated from the relative thickness with the formula (1); this strain is negative.

$$\varepsilon_z = \mathrm{Ln}(t/t_0) \tag{1}$$

where t_0 is the initial thickness, t is pole thickness of the deformed disk.

Calculation hypotheses

- The material is homogeneous and isotropic.
- First, the disk radius is considered as constant along the disk thickness
- The disk is deformed as a membrane.

  – Strains in the disk plane near its pole.

  $$\varepsilon_\varphi = \varepsilon_\theta \tag{2}$$

  – Cupola radii at the disk pole.

  $$\rho_\varphi = \rho_\theta = \rho \tag{3}$$

  – Stresses in the disk plane near its pole.

  $$\sigma_\varphi = \sigma_\theta = P\rho/(2t) \tag{4}$$

  where P is the gas pressure, t is pole thickness of the deformed disk, ρ is cupola radius at the disk pole.
- The volume of a metallic material is not modified by plastic deformations.

  $$\varepsilon_\varphi + \varepsilon_\theta + \varepsilon_z = 0 \tag{5}$$

Von Mises stress $\bar{\sigma}$ and strain $\bar{\varepsilon}$

The Von Mises stress $\bar{\sigma}$ and strain $\bar{\varepsilon}$ are calculated in order to compare the mechanical properties obtained with disk testing and with another mechanical testing.

$$\bar{\sigma} = \frac{1}{\sqrt{2}}\left[(\sigma_\phi - \sigma_\theta)^2 + (\sigma_\theta - \sigma_z)^2 + (\sigma_z - \sigma_\phi)^2\right]^{1/2}$$

$$\bar{\varepsilon} = \frac{\sqrt{2}}{3}\left[(\varepsilon_\phi - \varepsilon_\theta)^2 + (\varepsilon_\theta - \varepsilon_z)^2 + (\varepsilon_z - \varepsilon_\phi)^2\right]^{1/2}$$

$$(4) + \sigma_z \approx 0 \Rightarrow \bar{\sigma} = \sigma_\varphi = \sigma_\theta \Rightarrow \bar{\sigma} = \frac{P\rho}{2t} \quad (6)$$

$$(1) + (2) + (5) \Rightarrow \bar{\varepsilon} = 2\varepsilon_\varphi = 2\varepsilon_\theta \Rightarrow \bar{\varepsilon} = \mathrm{Ln}(t_0/t) \quad (7)$$

where P is the gas pressure, ρ is cupola radius at the disk pole, t is pole thickness of the deformed disk, t_0 is initial thickness of the disk.

Mechanical engineer properties

Frequently, the used tensile properties are not the true properties, the true stress σ and the true strain ε, but the engineer properties, the engineer stress S ($S = F/A_0$) and the engineer strain E ($E = \Delta L/L_0$); F is the tensile load, A_0 and L_0 are the original cross-sectional area and the original length of the specimen and ΔL is its absolute elongation.

During tensile testing, the local area reduction of the specimen appears from the load maximum or from the engineer stress maximum.

For biaxial testing, the engineer stress and strain are determined from the Von Mises true stress $\bar{\sigma}$ and strain $\bar{\varepsilon}$ with similar formula as for tensile testing.

- *Engineer stress S (Load per unit original cross-sectional area)*

$$S = \bar{\sigma}\frac{A}{A_0} = \bar{\sigma}\frac{t}{t_0}$$

$$(6) \Rightarrow S = \frac{P\rho}{2t_0} \quad (8)$$

- *Engineer strain E (Extension per unit original length)*

$$\bar{\varepsilon} = \mathrm{Ln}(1 + E)$$

$$(7) \Rightarrow E = \frac{t_0}{t} - 1 \quad (9)$$

Determination of the disk radius and thickness

The radius ρ and the thickness t of the deformed disk are needed to calculate the mechanical properties at the disk pole.

Disk deformation

If the disk is deformed as a spherical cupola, the pole radius ρ is the sphere radius; the external radius can easily be calculated from the deflection W by the geometrical relation (10).

$$\rho = (W^2 + A^2)/(2W) - r \quad (10)$$

where W is the deflection at the disk pole, A is internal radius of the disk embedding (Fig. 2), r is die radius at the disk embedding (Fig. 2)

The hypothesis of the spherical cupola has been verified by geometrical measurements on the deformed disk.

Thickness and strain at the disk pole

The pole strain is obtained from the deflection W with the formula (11) determined by analytical calculations of plastic strains. This theoretical result has been validated by measuring pole thicknesses of different disks made of various metals.

$$\varepsilon_{\phi i} = \int_0^{W_i} dh/\rho \quad \text{and} \quad \bar{\varepsilon}_i = 2\varepsilon_{\phi i}$$
$$\Rightarrow \bar{\varepsilon}_i = 2\int_0^{W_i} \frac{\left[1 - 2\,r/A\left(1/1 + (W^2/A^2)\right)\,\sin(2\,\mathrm{Arctg}(W/A))\right]}{\rho} dW \quad (11)$$

where W is the deflection at the disk pole, A is internal radius of the disk embedding, r is die radius at the disk embedding, ρ is radius of the disk deformed as a spherical cupola, ρ is radius calculated from the deflection with the formula (10).

Fatigue of disks

During disk fatigue testing, the deflections are small with the result that the maximum strain is located in the embedding zone; consequently, during the low cycle fatigue, the material is plastically deformed at the disk embedding while it is only elastically deformed at the disk pole. The prior calculations (Calculation method and Determination of the disk radius and thickness) must not be

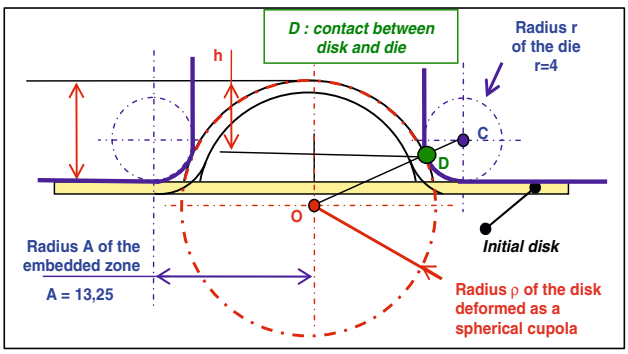

Fig. 2 Disk deformation—geometrical parameters. The deformed disk is considered as a sphere from the contact D with the die

used for fatigue testing because they accurately determined the mechanical properties only at the disk pole.

For low cycle fatigue, the number N of cycles to rupture is related to the cyclic plastic strain $\Delta\varepsilon_p$ with the law (12) proposed by Manson-Coffin [19]:

$$\Delta\varepsilon_p = AN^{-a} \quad (12)$$

If a monotonic rupture test (rupture strain ε_R) is considered as a fatigue test within 0.5 cycle, the Manson-Coffin law becomes:

$$\Delta\varepsilon_p = \varepsilon_R(N/0.5)^{-a} \quad (13)$$

At the pressurization beginning, the elastic stress and strain are calculated from the deflection W by the analytic formula demonstrated for membranes elastically stressed by uniform pressure [20]; so the deflection W_y is determined when the yield stress σ_y value is obtained; the yield stress σ_y may be measured by previous biaxial or tensile tests.

The plastic strain $\Delta\varepsilon_p$ depends on the deflection difference $(W - W_y)$; W is the deflection measured during the plastic deformation.

For the small deflection measured during fatigue tests, the strain $\Delta\varepsilon_p$ is linearly approximated against the deflection W:

$$\Delta\varepsilon_p = K(W - W_y) \quad (14)$$

For the disk fatigue tests, the deflection W is fitted against the cycle number N of rupture by the empirical law (15):

$$(W - W_y) = CN^{-c} \quad (15)$$

The coefficient K can be calculated from the formulas (12–15).

Experimental results

Several experimental results are presented in order to show the application ranges of the biaxial disk testing and the interests of the mechanical properties determination; thus, the material properties and the metallurgical phenomena are succinctly described and analysed.

Studied material

Disks are made of copper alloyed with small contents of other elements such as chromium and zirconium. First, the alloy is given in a solution-treatment; next, it is quenched to obtain a supersaturated solid solution at room temperature; a temper treatment at relatively low temperature creates fine and coherent precipitations from the unstable solid solution in order to obtain an important hardening.

Tensile specimens and disks have been machined from extruded bars.

Monotonic rupture of disks

The true mechanical properties (true stress–true strain law) of materials are calculated from defined hypotheses and particularly, the deformation must be uniform in the considered volume; thus, the true tensile properties are not easily calculated when the local area reduction has appeared.

For tensile tests, the area reduction begins when the load (or the engineer stress) has reached a maximum; this load maximum is reached for the uniform elongation E_u; the elongation E_u can be much smaller than the rupture elongation E_r.

Experimental pressure–deflection curves of disk testing

For disk testing, the experimental curves do not present a pressure maximum before the final rupture (Fig. 3) but only a decreasing of the pressure rate; rate decrease begins at the pressure P_u and at the deflection W_u; it corresponds to the end of the material uniform deformation; when a local deformation appears, the disk is no more deformed into a spherical cupola with the result that the measured deflection is greater than the theoretical sphere deflection.

NB: The pressure varies linearly depending on the deflection up to the pressure P_y; the pressure P_y defines the end of the elasticity behaviour.

The experimental range of the uniform plastic deformation (from P_y to P_u) is much wider than the elasticity range (from 0 to P_y); compared to tensile testing, the experimental results of disk testing expand the uniform plasticity range.

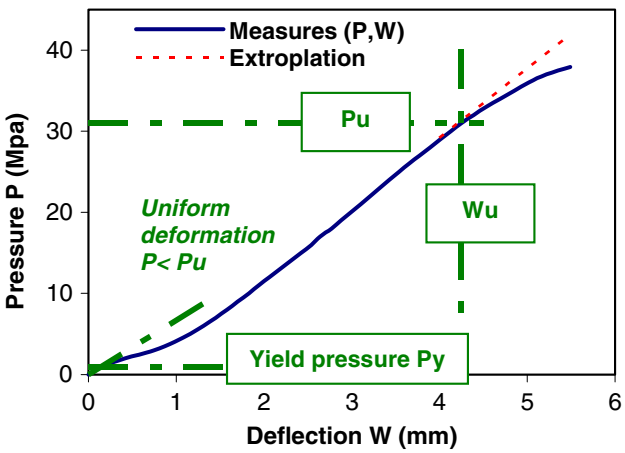

Fig. 3 Pressure–deflection curve. Low-alloyed copper at room temperature. At the highest deflections, the pressure rate decreases when the disk deformation is no more homogenous

Validity range of the calculated mechanical properties

From the experimental results (Fig. 3), the engineer stress S is calculated using the formula (8) and (10).

The engineer stress has been plotted depending on the deflection (Fig. 4); the results reveal different kinds of behaviour related to the validity of the calculation.

- *Beginning of plastic behaviour from the deflection W_y*

For deflections smaller than 1 mm, the results are not coherent since the stress S decreases as the disk becomes increasingly deformed.

For these small deflections, disk observations have shown that the material is plastically deformed in the embedding zone while the deformation is only elastic at the disk pole; the plastic deformation is consecutive to the flexion that has been neglected for the mechanical calculation. Since the deformation is heterogeneous, the cupola radius is different from the radius calculated for the theoretical sphere obtained with homogenous deformations.

The deflection W_y needed to obtain a 0.2%-plastic strain is calculated from the formula (11); the same value of the 0.2% is used to determine the yield strength from tensile testing.

- *End of the uniform plastic behaviour at the deflection W_u*

The engineer stress S reaches a maximum at the deflection W_u. For the greatest deflections, the calculated stress S decreases since the deformation is no longer homogeneous when the local area reduction occurs.

NB: The uniform deflection W_u calculated for the maximum of the engineer stress S is similar to the uniform deflection determined from the experimental curve (Fig. 3); *but the deflection W_u is more reliably determined from the numerical maximum of the engineer stress than from the beginning of the pressure rate decreasing.*

Mechanical engineer properties

When the hypotheses and the calculations are validated (deflections range from W_y to W_u), the engineer stress S and strain E are calculated with the formulas (8–11).

The proposed calculation method is validated to determine the material mechanical properties and the beginning of area reduction because the disk results are identical to the tensile properties (Fig. 5):

- the first engineer stress calculated for the deflection W_y corresponding to a 0.2%-plastic strain is similar to the tensile yield strength S_y obtained for the same plastic strain of 0.2 %,
- for the uniform deflection W_u, the engineer stress and strain reach maximal values that are identical to the tensile ultimate strength S_u and uniform elongation E_u.

True mechanical properties and mechanical behaviour

When the hypotheses and the calculations are validated (deflections range from W_y to W_u), the true stress $\bar{\sigma}$ and strain $\bar{\varepsilon}$ are calculated with the formulas (6), (7), (10) and (11).

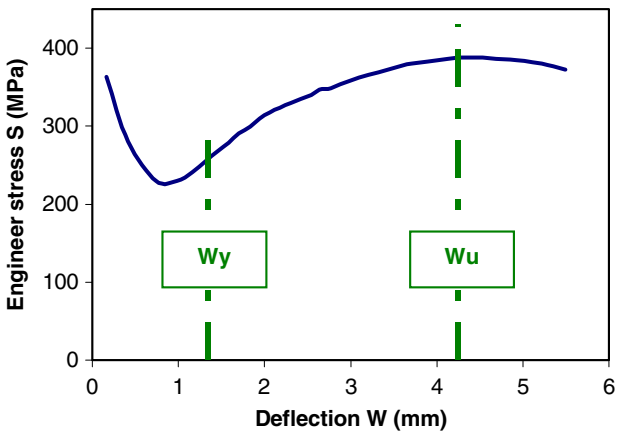

Fig. 4 Nominal stress versus deflection. Low-alloyed copper at room temperature. For deflections smallest than 1 mm, the calculated stress is not valid because the embedding flexion has been neglected. The stress reaches a maximum for the deflection W_u when the deformation becomes localized

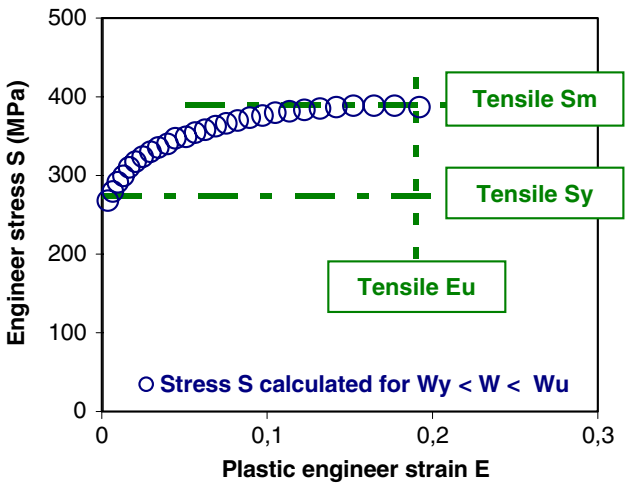

Fig. 5 Engineer mechanical properties. Low-alloyed copper at room temperature. The engineer mechanical properties (S_y, S_m, E_u) are identical with tensile testing and disk testing

The determined true properties (Fig. 6) show that the material behaviour can be modelled by the usual law proposed by Hollomon [17].

The exponent n of the Hollomon law is defined as the hardening index; for tensile testing, the value of the hardening index is identical to the maximum uniform true strain ε_{max}.

For disk testing, the hardening index is also identical to the maximum true strain (Fig. 6); again, this result validates the method proposed to calculate the mechanical properties and to determine the beginning of area reduction.

NB: If the beginning of area reduction has not been determined, the mechanical properties could be calculated for deflections greater than W_u until the rupture of the disk. At these great deflections, the results would not be valid because the formula (11) must not be used for heterogeneous disk deformations; we notice that these invalid results are not fitted by the Hollomon law obtained for homogeneous material (Fig. 6).

Moreover, if the results obtained at the greatest deflections had been used to determine the hardening law, the hardening index would have been smaller than the maximum strain.

Influence of temperature

At low strain rate, the ultimate strength S_u and the yield strength S_y as well as the uniform elongation E_u are similar for a disk and for a cylindrical tensile specimen machined from the same bar (Figs. 7 and 8). But, the biaxial tests have been performed at higher temperatures than those allowed by tensile tests when restricted by the mechanical extensometer.

The ultimate tensile strength S_u decreases when the temperature increases; this decreasing may be related to material softening by re-crystallization or by over-aging.

When the temperature increases, the uniform elongation E_u decreases; localized deformations are initiated by material heterogeneities; these heterogeneities appear more easily at the highest temperature.

Influence of strain rate

Cylindrical specimens have been used for tensile tests at different elongation rates (maximal ratio of 100); disks have been pressurized with larger ranges of loading rates (maximal ratio of 10,000).

At ambient temperature, the ultimate strength S_u increases as a function of the strain rate (Fig. 9); this usual result is related to the material visco-plasticity.

At the lowest loading rates, the ultimate strength is similar with both testing methods.

At the highest rates, the ultimate strength is lower for the tensile specimen. This difference may be related to edge effects: for a tensile specimen, the edges are stressed and a defect (second phase, machining defect...) creates stress concentration; the stress concentration initiates the area reduction at relatively low load.

At high strain rate, an edge defect concentrates the stress and initiates the rupture as the notch in the specimen of impact testing.

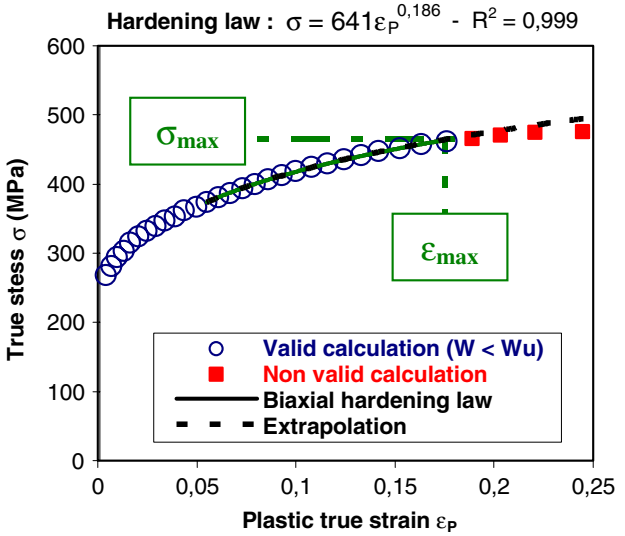

Fig. 6 True mechanical properties. Low-alloyed copper at room temperature. The hardening index (exponent of the hardening law) is similar to the strain maximum as for tensile testing

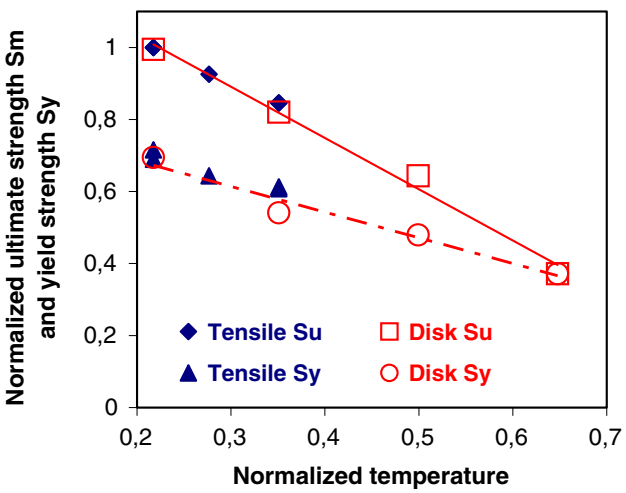

Fig. 7 Mechanical resistance versus temperature. Low-alloyed copper. The ultimate strength and the yield strength are identical with tensile testing and disk testing

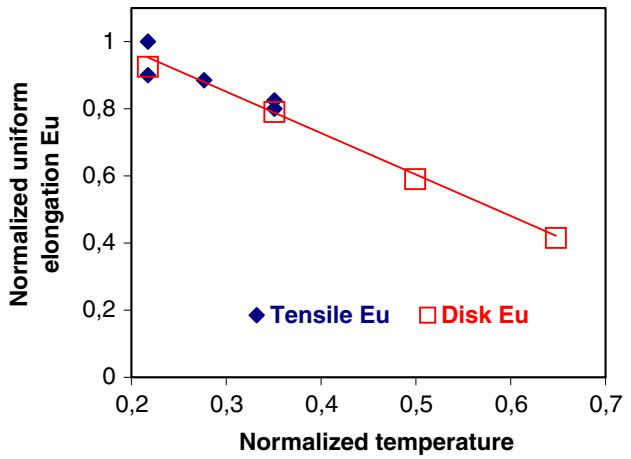

Fig. 8 Uniform elongation versus temperature. Low-alloyed copper. The uniform elongation is identical with tensile testing and disk testing

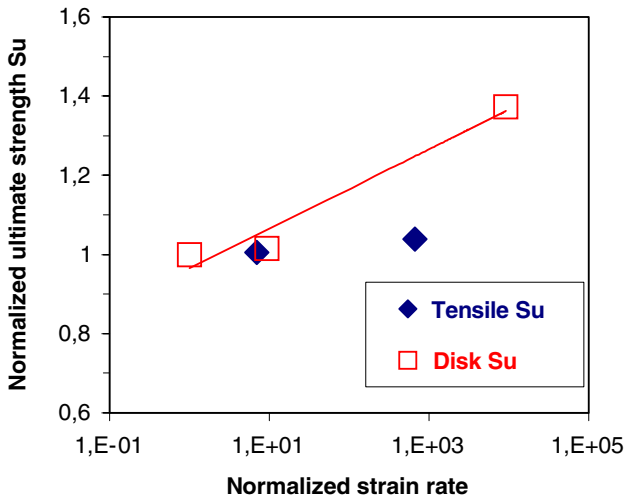

Fig. 9 Ultimate strength at different strain rates. Low-alloyed copper at 20 °C. The resistance increases as a function of the strain rate; this behaviour is related to the material visco-plasticity

The disk is embedded with the result that the edges are not located in the deformed zone and their defects are not stressed.

As a result of stressing without edge effects, disks tests may be performed at high temperature and at high strain rates (Fig. 10); for these extreme parameters values, the tensile results are commonly too scattered to be exploited.

Creep testing of disks

Mechanical loading of the disk

While the pressure remains constant (Fig. 11), the deflection W increases with the result that the cupola

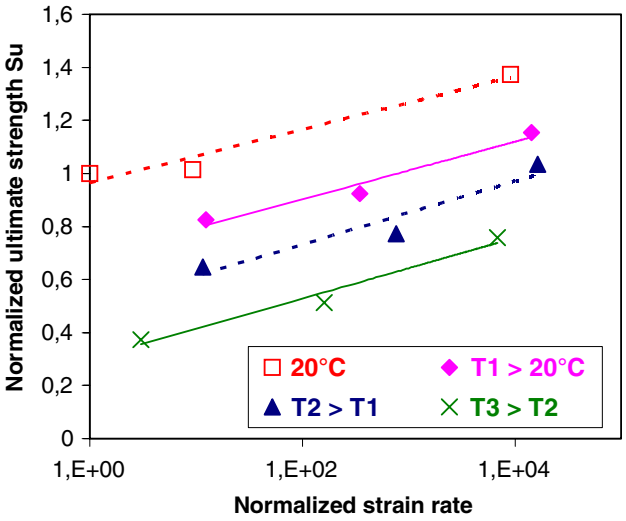

Fig. 10 Ultimate strength at different temperatures and different strain rates. Low-alloyed copper. Disk tests may be performed within very large ranges of temperatures and strain rates

radius decreases; consequently, the engineer stress S decreases.

$$S = \frac{P\rho}{2t_0} \quad d(\rho/t_0)/dW < 0 \Rightarrow dS/dW < 0$$

But when the radius decreases, the disk deformation increases and the disk thickness decreases; consequently, the stress $\bar{\sigma}$ remains about constant during the entire creep test for the used deflections (Fig. 11).

$$\bar{\sigma} = \frac{P\rho}{2t} \quad d(\rho/t)/dW \# 0 \Rightarrow d\bar{\sigma}/dW \# 0$$

W is the deflection, ρ is radius of the spherical cupola, t_0 is initial thickness of the disk, t is thickness of the deformed disk.

In conclusion, the disk creep method is experimentally validated because the stress is about constant during the secondary creep.

Typical results: creep testing of austenitic steels

The true strains are calculated with the formula (7), (10) and (11); the strain evolution (Fig. 12) reveals the usual creep phases [18]:

- *the primary creep* when the strain rate decreases,
- *the secondary creep* at constant strain rate $\dot{\varepsilon}_{II}$,
- *the tertiary creep* when the strain rate quickly increases until the rupture.

The secondary creep rate $\dot{\varepsilon}_{II}$ is calculated by a linear fitting of the experimental strains.

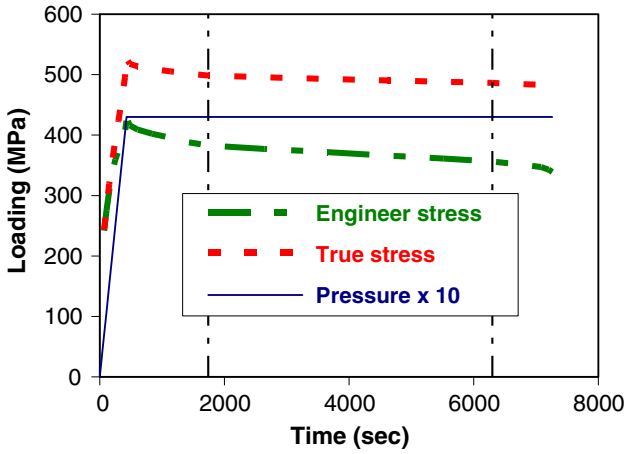

Fig. 11 Disk loading during creep testing. Austenitic steel. During creep testing of disk, the true stress is about constant during the secondary creep (See Fig. 12)

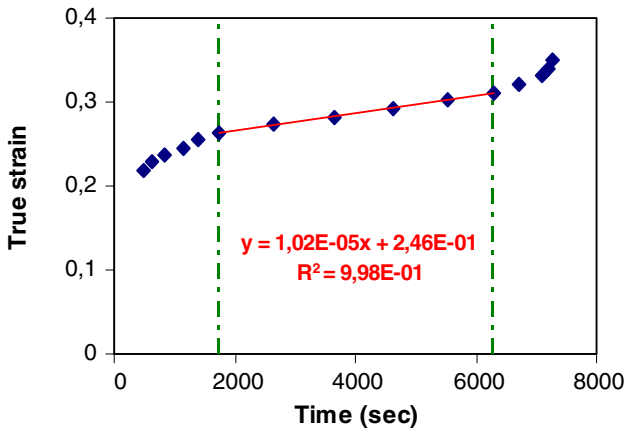

Fig. 12 Creep testing of disk. Austenitic steel. For the tested austenitic steel, the 3 usual creep phases are revealed, especially the secondary creep at constant strain rate

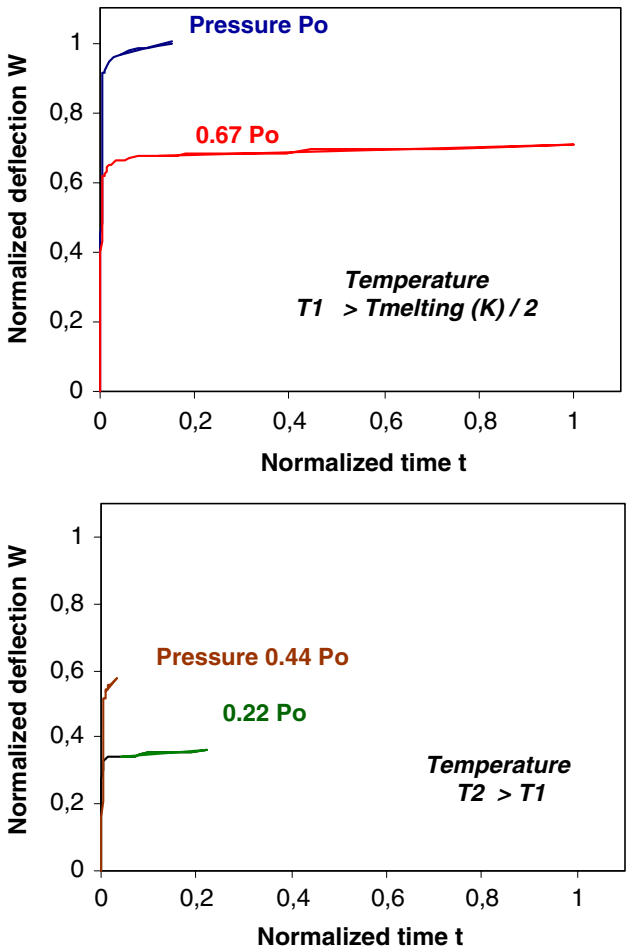

Fig. 13 Creep testing of disk. Low-alloyed copper. Each test has stopped during the secondary creep when crossing cracks have been developed

Creep testing of the low-alloyed copper

For the low-alloyed copper previously studied, all the creep tests performed at different temperatures have been stopped before the tertiary step (Fig. 13) because crossing cracks have appeared during the secondary creep; these cracks create leakages that prevent further pressurisation of the disks.

When the leakage is detected, crack length is equal to the thickness of the disk and, in consequence, is small; this damage should be revealed for greater crack lengths if the creep specimens are thicker than the disks.

Micrographic observations

Micrographs have revealed inter-granular cracking in disks tested at high temperature (Fig. 14b); before cracking, thickenings of grain boundaries have been observed (Fig. 14a).

Low cycle fatigue of disks

Different fatigue tests have been performed with the same low-alloyed copper:

- disk testing: samples (0.75 mm-thickness) are alternatively and symmetrically pressurized on both faces,
- compression-tension: cylindrical specimens (8 mm-diameter) are loaded by symmetrical compression-tension elongations,
- triangular samples (2 mm-thickness) are deformed in flexion with symmetrical deflections.

Fatigue lives found with the three testing methods are slightly different because of mechanical loadings and the thickness of the specimens (Fig. 15):

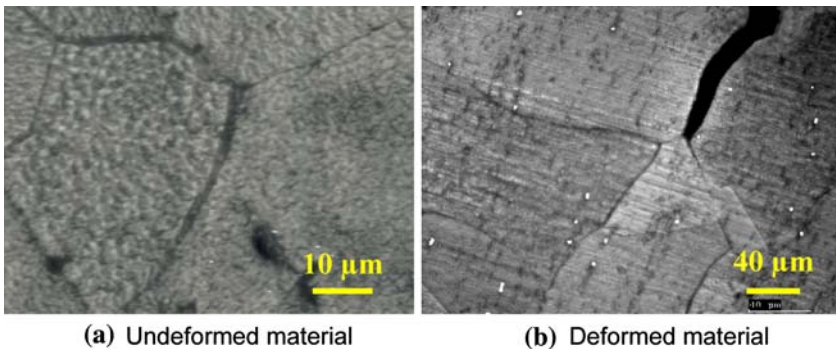

Fig. 14 Micrographs of disks after creep testing at high temperature. Low-alloyed copper. After heating, the grain boundaries become thick (**a**); cracks are initiated in the thick boundaries during the disk test (**b**)

- as the specimens are not perfectly homogeneous and isotropic, buckling has occurred from the very first cycles of tension-compression; thus, the strains could not have been precisely determined because they were localized,
- the disk testing creates asymmetrical strain cycles $(\varepsilon_t + \varepsilon_f/\varepsilon_t - \varepsilon_f$ where ε_f is the flexion strain and ε_t the tension strain) while the loading is symmetrical for both the other testing methods,
- the thickness of the specimens influences the crack initiation and propagation:
  - the initiation is easier for the thin disk than for the thicker specimens used for tension and flexion studies because stress concentration is more important,
  - edge defects initiate the crack in the flexural specimens while they are not loaded in the disk,
  - the propagation phase is shorter in the thin disk than in thicker specimens used for flexion or tension.

NB: The differences (Fig. 15) *between the three testing methods remain smaller than the scattering usually obtained with a single testing method of low cycle fatigue.*

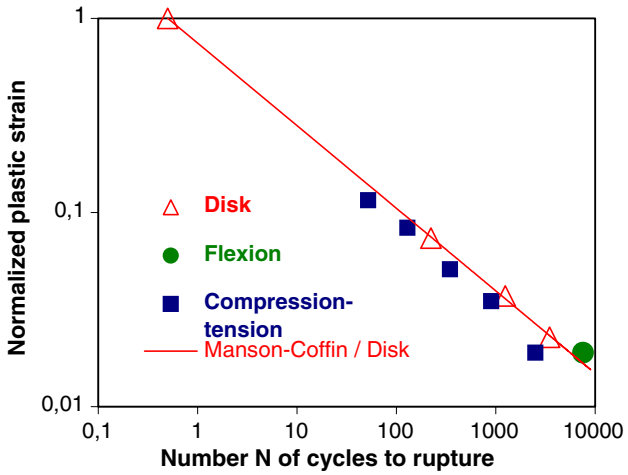

Fig. 15 Low cycle fatigue. Low-alloyed copper. Fatigue life is about similar with the 3 testing methods

Discussion

Thermo-mechanical properties of the low-alloyed copper

After its artificial ageing, the low-alloyed copper is unstable at medium and high temperature; it may evolve to obtain a more stable structure by diffusion of solute atoms with the result that new phases may appear or existing phases may grow.

Micrographs reveal this metallurgical evolution that produces quasi-continuous inter-granular phases.

The inter-granular phases create a microscopic embrittlement because they initiate cracking; they also create a macroscopic embrittlement because they simultaneously reduce both the ultimate strength and the uniform elongation.

The inter-granular cracking also creates leakages during the creep testing.

The phase apparition or evolution are related to the diffusion of the atoms. At intermediate temperature, this diffusion is localized near the grain boundaries because they correspond to microstructures without coherence and cohesion that magnify diffusion of the solute atoms.

The diffusion is thermally activated; because of this thermal activation, inter-granular cracking and gas leakage appear more easily when the temperature is increased.

The diffusion phenomena can be studied by tensile testing but the scattering related to the edge effects may mask the coherence of the results.

Moreover, the sensitive mass spectrometer detects fine leakages related to fine cracks and the length of the shortest detected cracks is the disk thickness; thus, fine and short cracks cannot be easily detected by tensile tests especially if the results are scattered.

Applications of disk testing

For instance, in a thermal exchanger under fluid pressure, thin walls and thicker parts are juxtaposed. The geometry

of the exchanger and thermal cycles create different thermo-mechanical loadings:

- very rapid heating (or cooling) creates important thermal gradients between the thin walls and the warmest and thickest parts; consequently, high gradients of thermal strains appear; because the thin walls are embedded by the thickest parts, their expansion initiates bulging; this bulging is magnified by the differential pressure applied to the wall and initiates wall cracking after several thermal cycles.
  Wall bulging is perfectly reproduced by disk deformation under gas pressure.
- when the thermal exchanger is used at high stabilized temperature, the thin wall is loaded by the differential pressure; the same loading is used during disk creep testing.

The disk testing can be used for other applications when material damage may be initiated by thermal cycles with large temperature amplitude or rate: furnaces for heat treatments, expansion bellows, equipments for chemical industry, aeronautic and spatial engines...

In particular, detection of very fine leakage through the disk is interesting in studying the damage and the imperviousness of thin walls.

The disk pressure testing can also be used to determine the formability of thin sheets at various deformation rates; the proposed calculation method clearly identifies the uniform deformation range; naturally, this deformation range is needed to determine the formability of materials.

As the specimen edges are not stressed during the test, disk testing presents several advantages:

- machining defects do not initiate localized deformations and the results are low-scattered. Consequently, disk results are reliable and reproducible while metallurgical phenomena are easily revealed,
- disk testing simulates the loading of real structures when thin walls embedded by thick zones are not subject to edge effects.

Ranges of temperature and strain rate

Disk tests can be performed up to 900 °C; such temperatures cannot be reached by oil bulging.

At the highest pressure rates, the disk rupture is obtained with durations much shorter than 1 s; the strain rate of disks reaches $10^0 s^{-1}$; this maximal strain rate is much smaller than the rates obtained by mechanical or explosive loadings but disk testing at high rate can be easily performed and exploited within the whole temperature range up to 900 °C.

Sensitivity of disk testing

Prior results have shown that disk testing is sensitive to microscopic evolutions such as the inter-granular precipitation in low-alloyed copper.

Other studies have demonstrated high sensitivity to other microscopic parameters: disks made of nickel alloy have been pressurized until rupture without anomalies in their mechanical behaviour [10]; but the mass spectrometer has detected helium leakage for pressures lower than 10% of the rupture pressure; these leakages have been related to crossing cracks due to metallurgical evolutions at high temperature; these evolutions could not be revealed by other mechanical testing as tensile testing because, unlike low-alloyed copper, they were too small to modify mechanical behaviour.

Disk testing is sensitive to parameters of the micrographic structure as specimen thickness is small; disk thickness is similar to the size of the metallurgical heterogeneities.

However, because of disk and cell geometries, the plastic range of the experimental curves is very dilated; for low-alloyed copper, the plastic range exists for pressures within a large range (ratio greater than 15, Fig. 3) while the corresponding strength evolves within a range 10 times smaller (Fig. 4). The plastic range dilatation may show small differences between materials while their mechanical behaviour seems similar if studied by other techniques.

Conclusion

The analytical method proposed in this paper is validated to calculate disk mechanical properties because they are identical to tensile properties. Disk creep testing gives coherent results; the fatigue life of disks is identical to the fatigue life measured in tension-compression and in flexion.

For monotonic rupture testing, disk deformation must be uniform to validate the calculation of material mechanical properties; the analytical method of calculation clearly demonstrates the range of uniform deformation with the result that mechanical behaviour of material can be correctly identified.

However, uniform deformation is needed to determine the plastic formability of sheets and this property is not easily provided by the usual oil bulging of membranes.

With the same equipment and with similar specimens, tests can be performed within a large range of temperature, from 20 °C up to 900 °C at ISMEP's laboratory and down to –196 °C in other laboratories. Naturally, the temperature range is far narrower with oil bulging tests.

The range of strain rate is also particularly wide (10^6–10^0 s^{-1}). Such wide ranges are obtained only with different mechanical loadings of tensile specimens: constant

loading, increasing loading applied by mechanical or hydraulic systems, impact loading.

The extreme values of the parameters can be simultaneously chosen for the same test; thus, a disk test can be performed at high temperature and at high strain rate.

Since the disk edges are not stressed, the disk results are very reproducible even if the tests are performed at high strain rate or/and high temperature.

Cell geometry and particularly, small disk thickness give very sensitive results.

Correct reproducibility and high sensitivity are needed to reveal the influence of fine defects or heterogeneities; the detection of helium leakages through the disk may be used to reveal light metallurgical evolutions; these evolutions create relatively short cracks while the macroscopic mechanical properties may not be modified.

If disk testing is particularly well adapted to studying the material properties of thin sheets or walls, it can also be used to determine more reliably the mechanical properties and behaviour of materials within the entire ranges of strain rate and temperature.

The proposed analytical calculation can be used to identify the required parameters values of thermomechanical modelling; in the future, these values can be optimized by numeric methods.

References

1. Fidelle JP, Broudeur R, Roux C (1975) Les essais de disques sous pression. Ivry, France, Mai 1975, Ed. C.E.A
2. Fidelle JP (1985) Present status of the disk pressure test for hydrogen embrittlements. 2nd A.S.M. symposium on hydrogen embrittlement. Los Angeles, USA, Mai 1985
3. Fidelle JP, Jouinot P, Stasi M, Barthelemy H (1994) The range of application of disk pressure test. 5th international conference on hydrogen effects on material behaviour. Jackson Lake, USA, Sept 1994
4. Barthelemy H, Pressouyre G (1985) Hydrogen gas embrittlement of steels. European Economic Community, Report EUR 9730EN, Bruxelles, Belgium
5. Gas containers. Cylinders and containers for compressed hydrogen. Test method for selecting construction materials. French standard NF E 29–732, Oct 1990
6. Vibrans G, Speitling A (1988) Investigation of hydrogen induced cracking of tempered 35CrMo4 during disk pressure test. 4th international conference “Hydrogen and materials”. Beijing, China, May 1988
7. Bachelet EJ, Troiano AR Hydrogen gas embrittlement and disk pressure test. Report NASA CR 134551, USA
8. Gantchenko V, Jouinot P, Stasi M (1999) Mechanical properties and failure analysis of metals and plastics cut off from a sheet or a vessel thin wall. EMAS, UK, Milano, Italy
9. Gantchenko V, Jouinot P, Stasi M (1999) Etudes de matériaux par des essais de disques sous hélium, une technique sensible et performante. Matériaux et Techniques, Déc 1999
10. Genevois-Stasi J (1998) Etude de l’évolution des propriétés mécaniques et métallurgiques de l’inconel 625 au cours du vieillissement, utilisation de l’essai de disques sous pression de gaz. Thèse, Paris 6, Juin 1998
11. Boulila A (2000) Etude expérimentale et modélisation numérique du gonflement hydraulique des plaques minces. DEA de Mecanique Appliquee, Ecole Nationale d’Ingenieurs de Tunis, Tunisie
12. Hill R (1950) A theory of the plastic bulging of a metal diaphragm by lateral pressure. Phil Mag, Ser 7, 41(322):1133
13. Mesrar R (1991) Comportement plastique des tôles sous sollicitation biaxiale et analyse numérique de la mise en forme par gonflement hydraulique. Thèse, Metz, 1991
14. Boulila A, Ayadi M, Zghal A, Jendoubi K (2002/3) Validation expérimentale du modèle de calcul en calotte sphérique de plaques circulaires minces sous l’effet d’un gonflement hydraulique. Mécanique et Industries
15. Jouinot P, Gantchenko V, Stasi M, Azou P (1988) High pressure disk test aided by computer. 4th international conference “Hydrogen and materials”. Beijing, China, Mai 1988
16. Jouinot P (1991) Développement de l’essai de disques sous pression. Applications à la fragilisation par l’hydrogène d’aciers faiblement alliés. Thèse, Paris 6, Déc 1991
17. Francois D (1996) Essais mécaniques des matériaux, Détermination des lois de comportement. Techniques de l’ingénieur M120, ETI, France
18. Saint-Antonin F (1995) Essais de fluage. Techniques de l’ingénieur M140, ETI, France
19. Rabe P, Lieurade HP, Galtier A (2000) Les essais de fatigue. Techniques de l’ingénieur M4171, ETI, France
20. Timoshenko S, Woinowsky-Krieger S (1959) Theory of plates and shells. McGraw-Hill Book, Company, Inc.